Phonon Scattering from Ferroelectric Domain Walls: Phonon Imaging in KDP

M. A. Weilert, M. E. Msall, A. C. Anderson, and J. P. Wolfe

Physics Department and Materials Research Laboratory, University of Illinois at Urbana-Champaign, Urbana, Illinois 61801

(Received 1 February 1993)

The ferroelectric domain wall is an ideal interface for studies of the boundary scattering of high frequency acoustic phonons. These internal interfaces have no contamination and can be reversibly created and destroyed by application of an electric field at the phase transition—122 K in KDP. Images of phonons in single- and multiple-domain cases show remarkable differences in the ballistic heat flux. Theoretical modeling based on acoustic wave reflection reveals that the domain walls act as nearly perfect grain boundaries.

PACS numbers: 66.70.+f, 63.20.Mt, 68.35.Gy, 77.80.Dj

The transport of thermal energy across crystalline boundaries has great practical importance, yet there are few cases where measurements agree with microscopic models of the interface. The classic example is the anomalously high thermal boundary conductance observed between a crystal and liquid helium, as first reported by Kapitza [1]. Also, at temperatures of a few kelvin the thermal conductance across solid-solid interfaces is generally not well described by acoustic-mismatch theory [2]. These large discrepancies are generally attributed to diffusive scattering of phonons by defects at the interface [3]. Acoustic-mismatch theory, in contrast, computes the transmission and reflection coefficients of an elastic wave under the assumption that $k_{\parallel}$, the wave vector parallel to the interface, is conserved (i.e., Snell's law), which is the condition for specular scattering [4]. While there are some notable exceptions [5], this condition is difficult to satisfy at ordinary (imperfect) interfaces for phonons with wavelengths of a few hundred angstroms or less. In this paper, we report the observation of scattering of high frequency phonons from "internal" interfaces—ferroelectric domain walls in KDP—and find that these interfaces act as nearly perfect "specular" interfaces. Our phonon imaging experiments provide detailed information about the propagation of all phonon modes, leading to an understanding of unusual anisotropies observed in the thermal conductivity of this crystal at low temperatures.

At room temperature KDP is a paraelectric material that has applications in nonlinear optics, principally as an efficient frequency doubler of laser photons, and in electro-optic devices [6]. The crystal symmetry about 122 K is tetragonal [7]. At $T = 122$ K, KDP undergoes a ferroelectric phase transition, in which domains of opposing electric polarization spontaneously appear, as shown in Fig. 1(a) [8]. The positive energy needed to create domain walls between regions of opposing polarization is more than offset by the reduction in overall electrostatic energy. If, however, the crystal is placed in an electric field greater than about 1 kV/cm along the fourfold axis as it passes through the transition, a single domain is formed, which persists at lower temperature even when the field is removed.

There is a structural change from tetragonal to orthorhombic which accompanies the ferroelectric phase transition [the actual distortion is much smaller than that shown in Fig. 1(a) ($< 1\%$)]. The separation of the planar domain walls is typically 3–10 μm. The change to single- or multidomained is controlled by cycling the crystal through 122 K with or without field, providing a useful system for studying the interaction of phonons with domain walls.

Our initial experiments with this crystal were thermal conductivity measurements over the temperature range 0.1–10 K. The principal results, to be reported in detail

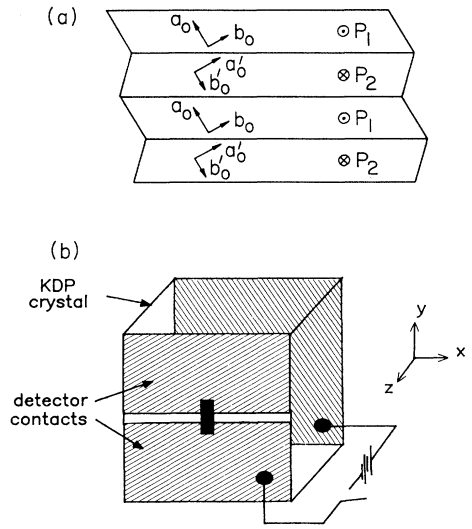

FIG. 1. (a) Diagram of the deformation of the KDP crystal structure at the ferroelectric transition. The orthorhombic unit cell is given by the basis vectors $\mathbf{a}_0$ and $\mathbf{b}_0$. Multidomain KDP forms when the sample is cooled in the absence of an applied electric field. Planar domains with a typical thickness of 3 to 10 μm have alternating polarization $\mathbf{P}$ and rotated orthorhombic structure. (b) Diagram of the sample and electrical connections. Shaded areas are copper films; the dark strip on the center of the near face represents the granular Al phonon detector.

0031-9007/93/71(5)/735(4)$06.00

elsewhere [9], show a distinct anisotropy in the thermal conductivity linked with domain wall scattering: (a) The thermal conductivity along the [100] axis for a multidomain sample is 30% less than that for a single-domain sample, and (b) the domain walls cause a 40% drop in the thermal conductivity along [110]. To investigate the details of this anisotropic phonon scattering from domain walls, we employ the phonon imaging technique [10] described below.

The present experiments utilize a strip of granular aluminum (10×30 μm^2) with a superconducting transition centered at 1.7 K as a phonon detector. The electrical contacts to this bolometer are 2000 Å thick copper pads evaporated over most of the crystal face which also act as one of the poling electrodes, as shown in Fig. 1(b). The opposite (001) face is completely covered with a 2000 Å copper film which acts as both the other poling electrode and the absorbing medium for the 15 ns Ar^+ laser pulse. These pulses, with an energy of roughly 7.5 nJ focused onto the Cu film ($R_{spot} \approx 20$ μm), produce a local heated region of about 10 K, corresponding to a Planck distribution of phonons with a peak at 600 GHz. Figure 2 shows ballistic heat pulses propagating along the [001] direction in a 3 mm thick KDP crystal at 1.7 K. We see that the relative intensities of the longitudinal (L) and transverse (T) modes depend upon whether the crystal is single domain or multidomain.

By raster scanning the laser beam across the (001) surface and recording the output from a boxcar averager, which integrates the signal over the time gate shown in Fig. 2, a phonon image is produced in which the bright areas correspond to intense heat flux. The phonon image shown in Fig. 3(a) is obtained for the single-domain case and contains a distinct pattern of phonon caustics, arising from the phonon focusing effect [11,12]. By taking a series of images with a narrow time gate, we have empirically identified the structures associated with the fast transverse (FT) and slow transverse (ST) modes, as indicated in the figure. The L mode produces no caustics. The sample is now warmed up to above 122 K and cooled back to 1.7 K without applying an electric field. The resulting multidomain crystal exhibits a markedly different phonon image, shown in Fig. 3(b). By observing the scattering of white light through the crystal, we ascertain that the domain walls have arranged themselves in horizontal planes, whose projections on the phonon image are a series of closely spaced horizontal lines [as in Fig. 1(a)].

The single-domain pattern [Fig. 3(a)] exhibits the symmetry expected of an orthorhombic crystal slightly distorted from tetragonal symmetry: A twofold axis replaces the fourfold axis of tetragonal symmetry. If the crystal is poled with an electric field of the opposite sense, the pattern rotates by 90 deg about the center and the electric polarization reverses sign. The transit of phonons through alternating electric polarization domains in the multidomain sample modifies the symmetry of the pho-

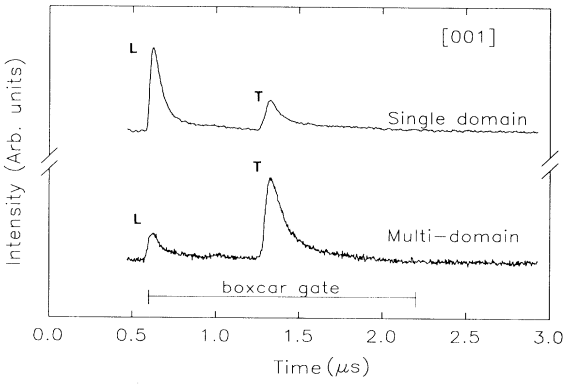

FIG. 2. Time trace of bolometer response for phonons propagating along [001] in single-domain and multidomain KDP. (Time is measured from the 10 ns laser excitation pulse.) Distinct L and T phonon arrivals are visible, but the relative intensities change in the presence of the domain walls. The traces are scaled to the same maximum intensity.

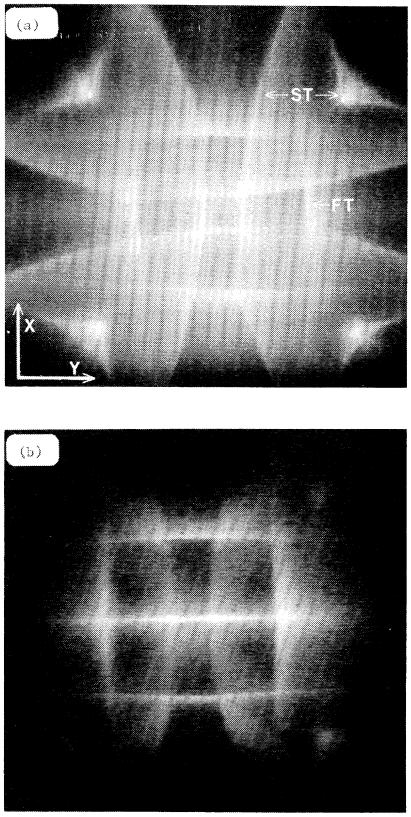

FIG. 3. Experimental phonon images of KDP including both fast and slow transverse phonon arrivals: (a) single domain image; (b) multidomain image. The FT caustic pattern of the multidomain image has been electronically enhanced to increase visibility.

non images as shown in Fig. 3(b). These experiments show unequivocally that the interaction of phonons with the domain walls is highly dependent upon phonon polarization and mode.

In order to analyze the anisotropic scattering by domain walls, it is first necessary to determine the wave vector, **k**, and the polarization, **e**, of the phonons which comprise all parts of the phonon focusing pattern of Fig. 3(a). We have devised a simple scheme for dealing with the nine unknown elastic constants of the orthorhombic crystal. These constants originate from a splitting of three of the six elastic constants for tetragonal ($T > 122$ K) KDP, which are known [13]. We symmetrically split C_{11}, C_{13}, and C_{44}, all by the same percentage, and use this percentage splitting as an adjustable parameter to fit the experimental phonon focusing pattern. The remaining three tetragonal constants (C_{12}, C_{33}, and C_{66}) are left unchanged. We find that a 5% splitting gives a quite reasonable representation of the experimental focusing pattern, as shown in Fig. 4(a). This is a Monte Carlo calculation which simulates the propagation of an isotropic distribution of wave vectors, whose group velocities are computed by the elasticity theory [14].

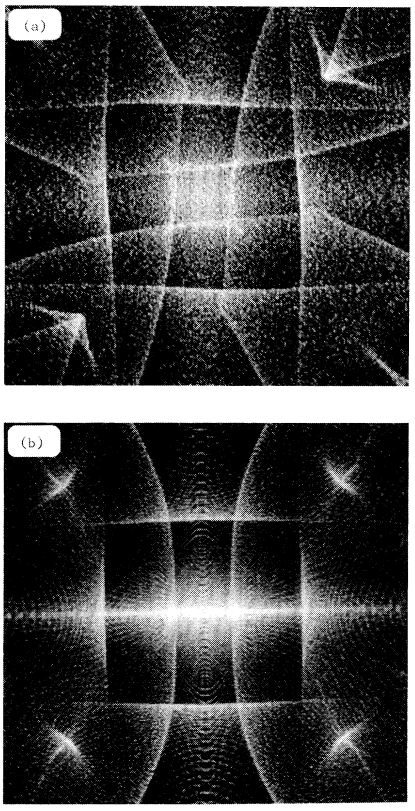

FIG. 4. Computer generated phonon images of KDP, using 5% split elastic constants: (a) single domain image; (b) multidomain image.

Having a reasonable representation of the phonon propagation in the orthorhombic KDP crystal, we now approach the problem of scattering at the domain walls. We start with a phonon of wave vector **k** at the heater surface, calculate its group velocity **V**, and propagate it until it strikes a domain wall. An acoustic mismatch occurs at the interface because two portions of the same type of crystal with different orientations are joined together. Knowing the orthorhombic distortion, we calculate the transmission and reflection coefficients for the three transmitted and three reflected waves having the same $k_{\|}$, using the 5% split elastic constants [4]. Fortunately, for a particular starting $k_{\|}$, the resulting chain of phonon interactions with the surface have only two sets of reflection and transmission coefficients, because $k_{\|}$ is conserved throughout the scattered trajectory. Starting with an isotropic distribution of phonons, we can produce a spatial image of the phonons which traverse the multidomain crystal and strike the detector surface. The result is shown in Fig. 4(b). This calculation reproduces all of the qualitative features of the experimental data in Fig. 3(b), indicating that the interaction between phonons and the domain walls is well described by an acoustic mismatch theory.

The details of the internal boundary scattering can be obtained by a closer inspection of the reflection and transmission coefficients for the different phonon modes. Figure 5 and the accompanying table summarize the results of this calculation. We take the image plane to be x-y and the domain-wall planes to be y-z. From the pho-

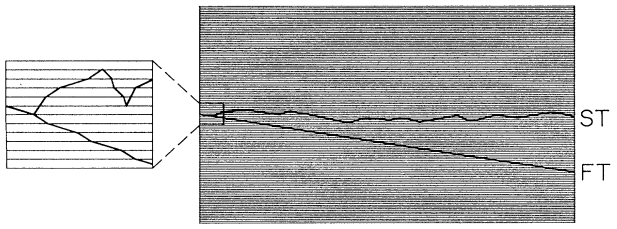

Phonons	Polarization	Reflection probability at a single wall	Net effect through crystal
Horizontal ST caustic	$\approx\underline{y}$	≈50% little mode conversion	Channeled
Vertical ST caustic	$\approx\underline{x}$	≈ 1% transmitted to ST	Near ballistic
FT caustic	$\approx\underline{z}$	<< 1% reflection	Near ballistic

FIG. 5. Ray picture of phonon propagation through a multidomain sample for an FT and an ST phonon which would both arrive at the same image point in the absence of domain wall scattering. The reflection probability for the ST phonon along this direction is almost 50%, so that it is channeled into the bright horizontal line on the multidomain images. In contrast, the FT phonon undergoes only small-angle scattering and arrives at an image point very near to the single domain image point. The table gives a summary of the reflection probabilities for these phonons.

non focusing calculation we know that phonons contributing to the nearly vertical ST caustics in Fig. 3(a) have an x polarization. These phonons have a strong (99%) probability of transmission into the same mode so that the position of these caustics, shown in Fig. 3(b), are almost the same as in the single domain image of Fig. 3(a). Likewise, the phonons contributing to the strong FT caustics have a high probability of transmission into the same mode. These two cases correspond to "near ballistic" phonons which are least affected by the domain walls, as indicated in Fig. 5. In contrast, the ST phonons contributing to the nearly horizontal caustics have a y polarization and are strongly (50%) reflected by a single domain boundary. Such phonons are "channeled" between several domain walls and give rise to the intense horizontal line at the center of Fig. 3(b).

It should be noted that the phonons in the multidomain phonon image have encountered several hundred interfaces before being detected, underscoring the fact that diffuse scattering at each of these interfaces is very weak. Thus, we find that the scattering of phonons from ferroelectric domain walls in KDP is well described by acoustic mismatch theory. The probability of a given phonon to reflect, transmit, or mode convert at the domain wall is highly sensitive to its mode, polarization, and direction of propagation. The phonon imaging method is a particularly effective means of elucidating these processes.

This work is supported by the National Science Foundation under the Materials Research Laboratory Grant No. DMR 89-20538 (M.E.M. and J.P.W.) and NSF DMR 89-19032 (M.A.W. and A.C.A.). The KDP crystal was obtained from Cleveland Crystals.

[1] P. L. Kapitza, J. Phys. (USSR) **4**, 181 (1941). A recent review is given by T. Nakayama, Prog. Low Temp. Phys. **12**, 115 (1989).

[2] A. C. Anderson, in *Nonequilibrium Superconductivity, Phonons, and Kapitza Boundaries,* edited by K. E. Gray (Plenum, New York, 1981); D. Marx and W. Eisenmenger, Z. Phys. B **48**, 277 (1982).

[3] E. T. Swartz and R. O. Pohl, Rev. Mod. Phys. **61**, 605 (1989).

[4] In an anisotropic medium, specular scattering at a boundary does not usually imply that the angle of incidence equals the angle of reflection.

[5] Examples where acoustic mismatch theory appears to hold for short-wavelength phonons are the interfaces between (a) liquid helium and an *in situ* cleaved NaF surface [J. Weber, W. Sandmann, W. Dietsche, and H. Kinder, Phys. Rev. Lett. **40**, 1469 (1978)], (b) liquid helium and *in situ* laser-annealed silicon [R. Wichard and W. Dietsche, Phys. Rev. B **45**, 9705 (1992)], (c) liquid helium and highly polished sapphire [G. A. Northrop and J. P. Wolfe, Phys. Rev. Lett. **52**, 2156 (1984)], and (d) a Ge crystal and an MgO film deposited at high temperature [C. Höss, J. P. Wolfe, and H. Kinder, Phys. Rev. Lett. **64**, 1134 (1990)].

[6] D. Eimerl, Ferroelectrics **72**, 95 (1987).

[7] R. J. Nelmes, Z. Tun, and W. F. Kuhs, Ferroelectrics **71**, 125 (1987).

[8] R. M. Hill and S. K. Ichiki, Phys. Rev. **135**, A1640 (1964).

[9] M. A. Weilert, M. E. Msall, A. C. Anderson, and J. P. Wolfe, Z. Phys. (to be published).

[10] G. A. Northrop and J. P. Wolfe, in *Nonequilibrium Phonon Dynamics,* edited by W. E. Bron (Plenum, New York, 1985).

[11] H. J. Maris, in *Nonequilibrium Phonons in Nonmetallic Crystals,* edited by W. Eisenmenger and A. A. Kaplyanskii (North-Holland, Amsterdam, 1986).

[12] G. A. Northrop and J. P. Wolfe, Phys. Rev. B **22**, 6196 (1980).

[13] O. Delekta and A. Opilski, Arch. Acoust. **5**, 181 (1980).

[14] G. A. Northrop, Comput. Phys. Commun. **28**, 103 (1982).

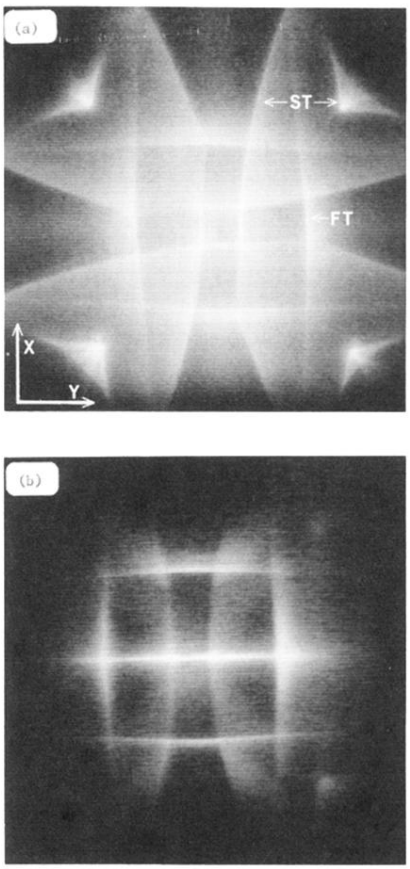

FIG. 3. Experimental phonon images of KDP including both fast and slow transverse phonon arrivals: (a) single domain image; (b) multidomain image. The FT caustic pattern of the multidomain image has been electronically enhanced to increase visibility.

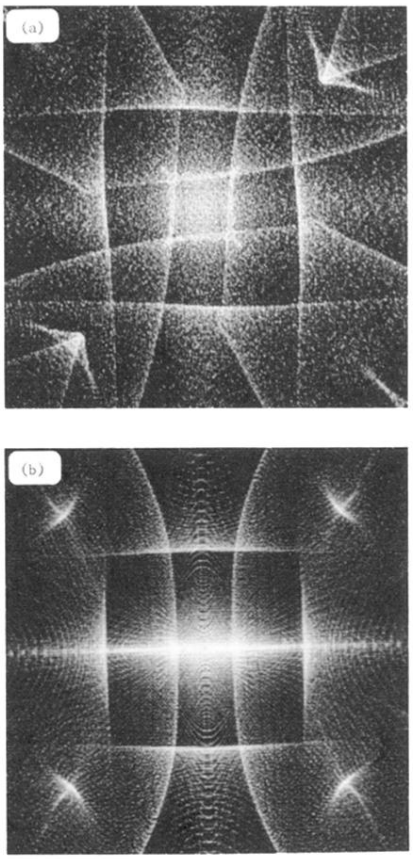

FIG. 4. Computer generated phonon images of KDP, using 5% split elastic constants: (a) single domain image; (b) multi-domain image.